Contact Angle Analysis, Surface Dynamics, and Biofouling Characteristics of Cross-Linkable, Random Perfluoropolyether-Based Graft Terpolymers

Jason C. Yarbrough,[†] Jason P. Rolland,[†] Joseph M. DeSimone,*[,†,§] Maureen E. Callow,[‡] John A. Finlay,[‡] and James A. Callow[‡]

Department of Chemistry, University of North Carolina at Chapel Hill, Chapel Hill, North Carolina 27599; School of Biosciences, The University of Birmingham, Birmingham B15 2TT, UK; and Department of Chemical and Biomolecular Engineering, North Carolina State University, Raleigh, North Carolina 27695

Received November 18, 2005; Revised Manuscript Received January 9, 2006

ABSTRACT: The conventional approach to prevention of marine biofouling has been the use of antifouling paints and coatings which function through the release of toxins in the immediate vicinity of the ship. Such technology, while admittedly effective, has proven to be responsible for an alarming increase in the levels of organotin and other toxic materials in and around dry docks, harbors, and shipping lanes which experience significant commercial and tourist traffic. Therefore, our objective is the rational design of minimally adhesive, mechanically stable, nontoxic fouling release coatings as responsible and practical alternatives to antifouling technologies. Herein we report on the synthesis and characterization of a series of cross-linkable perfluoropolyether (PFPE) graft terpolymers containing various alkyl (meth)acrylate monomers with glycidal methacrylate as the cure-site monomer. These materials were targeted for use as coatings to prevent marine biofouling. A series of terpolymers were prepared through application of the macromonomer approach, allowing for control of cross-link density, T_g, and modulus. Structure/property relationships were established through compositional variation with regard to the three classes of monomers. The first monomer class was an alkyl (meth)acrylate used to create the continuous phase of the microphase-separated graft terpolymers. Variation between methyl methacrylate (MMA) and *n*-butyl acrylate (BA) provided materials with a low (−10 °C) and a high (95 °C) T_g for the continuous phase. This was a means of isolating the effect of modulus and T_g on surface properties, while the basic chemical nature of the monomer remained unchanged. The second monomer class contained a curable functional group. Through incorporation of glycidyl methacrylate (GMA) in the monomer feed and manipulation of curing conditions, the relative effect of cross-link density on surface dynamics has been evaluated. The third monomer class was the PFPE macromonomer itself. The incorporation of this macromonomer was used to enhance the release properties of the resulting materials which relied on surface enrichment of the low surface energy PFPE component. Dynamic surface properties of these materials have been evaluated through dynamic surface tensiometry (DST). Herein, it has been demonstrated that contact angle hysteresis can be significantly mitigated (i.e., θ_r is maximized) by as much as 50° through variation in bulk polymer composition, the chemical nature of monomers, cross-link density, modulus, and environmental conditions at the time of cure. The antifouling and fouling-release potential of the experimental coatings were also evaluated by laboratory assays employing the green fouling macroalga *Ulva*. The results from these initial studies suggest promising antifouling properties, especially with regard to spore settlement which was strongly inhibited on the experimental surfaces. Additionally, those that did settle were only weakly attached with one sample set exhibiting fairly moderate release of the young *Ulva* plants.

Introduction

The performance of a material is often dictated by surface and interfacial properties, such as wettability, friction, and adhesion. These properties depend critically upon the molecular structure and composition at the surface or interface in question. It has been demonstrated that the composition and structure of the first one or two atomic layers at the interface are often quite different from those expected on the basis of bulk composition, but it is this surface composition which accounts almost entirely for the observed surface properties.[1,2] As such, there has been a tremendous effort to control polymer surface composition through external surface modification techniques (plasma, grafting, SAMs, etc.) as well as through bulk modification (blends, random and block copolymers, etc.).[3−7] The goal of bulk modification is generally the design of a polymer with a specific surface structure based on understanding, to some degree, of the tendency for surface enrichment of one component of a multicomponent polymer system.[8−12] This, however, presents some difficulties in that it is obvious that any such surface must be engineered with a particular set of environmental conditions in mind.

Among the various modern tools available for the analysis of surface dynamics, contact angle analysis and wetting techniques are considered standard methods for establishing the surface quality of a given material. Surface tensiometry methods are extremely sensitive probes of approximately the upper 0.5 nm of a surface and as such are among the most surface-sensitive techniques.[13,14]

The basic theory behind contact angle analysis is described by Young's equation. When a liquid drop is placed in contact with a surface, the liquid will form a contact angle (Figure 1) when the various interfacial tensions obey Young's equation

[†] University of North Carolina at Chapel Hill.
[‡] The University of Birmingham.
[§] North Carolina State University.
* To whom correspondence should be addressed: e-mail desimone@unc.edu.

10.1021/ma0524777 CCC: $33.50
Published on Web 03/14/2006

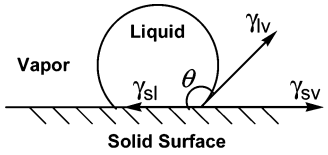

$$\gamma_{lv} \cos \theta = \gamma_{sv} - \gamma_{sl}$$

Figure 1. Young's equation for the static contact angle of a liquid drop on a solid surface.

as follows in Figure 1,[15] where γ_{lv}, γ_{sv}, and γ_{sl} are the surface tensions of the solid, liquid, and solid−liquid interface, respectively. Thus, the contact angle is related globally to (in fact, it is a manifestation of) the thermodynamic equilibrium of the three-phase system so described. In other words, the wettability of a surface is primarily a function of the surface free energy of both the solid and liquid phases. However, very few polymer surfaces strictly adhere to this theory as a consequence of the nonideal nature of any real surface. Fundamental assumptions in Young's equation are that the surface in question is homogeneous, smooth, and nondeformable (i.e., a static surface). However, in real systems the existence of a liquid−solid interface bears a host of possible consequences such as swelling of the polymer, liquid penetration, surface restructuring, and domain segregation, all of which serve to relax these theoretical constraints (i.e., a dynamic surface is nonideal). These phenomena, among others, are responsible for one of the biggest experimental difficulties found in the application of Young's equation, contact angle hysteresis. However, it is this deviation from ideal behavior which provides a convenient, albeit an indirect, measure of surface dynamics.

Herein we discuss the synthesis of a series of perfluoropolyether (PFPE) graft terpolymers which were designed to resist surface reorganization when brought into difficult environments. The wettability of these materials was studied as a function of bulk composition, cross-link density, modulus, and curing conditions as probed by dynamic contact angle analysis. PFPEs exhibit incredibly low surface energies (12−20 mN m^{-1}), very low glass transition temperatures (−120 to −70 °C), and remarkable chemical and thermal stability. Indeed, PFPEs are a unique class of materials which have flexibility similar to that of PDMS (poly(dimethylsiloxane)) owing to low barriers to rotation of the ether bonds, while offering the high chemical resistance and low surface energy of fluoropolymers via the strong C−C and C−F bonds.[16] For these reasons we have sought to explore PFPE-based platforms for a variety of applications including soft lithography, nanoparticle fabrication, and microfluidics.[17] The combination of low surface energy and flexibility makes PFPEs ideal candidates for highly surface active components of a random copolymer system.

Marine biofouling is a worldwide problem costing billions of dollars per year in transportation costs due to increased fuel consumption.[18] Biofouling has been controlled traditionally by biocidal antifouling paints, but increasingly stringent restrictions favor nonbiocidal approaches to the control of fouling. Commercial nonbiocidal coatings that facilitate only the weak adhesion of macrofouling organisms such as barnacles, tubeworms, and macroalgae are currently all based on silicone elastomers.[19−21] These fouling release coatings do not prevent the accumulation of fouling but have characteristics which facilitate its release under suitable hydrodynamic conditions. The fouling release properties of silicones are attributed to a number of factors, including low critical surface tension (∼23 mN m^{-1}),[22] coating modulus,[20,22,23] and thickness.[24]

Ulva (syn, *Enteromorpha*) is the most common macroalga that fouls ships and other submerged structures. Dispersal of *Ulva* is mainly through motile, quadriflagellate zoospores (approximately 7−8 μm in length), which are released in large numbers and which respond to a large number of settlement cues[25] and which rapidly germinate into sporelings (young plants). Inhibiting the settlement or adhesion strength of *Ulva* spores and sporelings would be a major factor in the control of fouling. The ease of removal of spores and sporelings can be measured by application of hydrodynamic forces using a water-jet apparatus[25] or a turbulent flow channel.[26,27]

The development of an environmentally friendly coating that is an improvement on current silicone technology would have wide application in the marine environment. This investigation examines the performance of perfluoroether-based terpolymer films with respect to (a) the settlement of *Ulva* zoospores and (b) the adhesion characteristics of *Ulva* spores and sporelings.

Experimental Section

Materials and Equipment. Methyl methacrylate (MMA, 99% Aldrich), *n*-butyl methacrylate (BMA, 99% Aldrich), butyl acrylate (BA, 99% Aldrich), hydroxyethyl acrylate (HEA, 99% Polysciences), and glycidyl methacrylate (GMA, 99%) were run through an alumina column before use. 2,2-Azobis(isobutyronitrile) (AIBN, 98% Aldrich) was recrystallized from methanol. *N*-(Aminopropyl)-methacrylamide hydrochloride (APMA, 99% Polysciences) and sodium ethoxide (21 wt % solution in ethanol, Aldrich) were used as received. The photoacid generator WPAG 336 was generously supplied by Wako Chemicals. 1,1,1,3,3-Pentafluorobutane (PFB) was purchased from Solvay Fluorides under the trade name Solkane 365 MFC and used as received. Tetrahydrofuran (THF, 99%), methyl ethyl ketone (MEK, 99%), α,α,α-trifluorotoluene (TFT, 99%), and methanol (MeOH, 99%) were purchased from Aldrich and used as received. Potassium bromide (KBr, 99%), sodium nitrate ($NaNO_3$, 99%), and sodium dichromate dihydrate ($NaCr_2O_7 \cdot 2H_2O$, 99%) were purchased from Aldrich, and saturated aqueous solutions were generated by adding the salts to water until a precipitate formed. Krytox methyl ester (average MW = 1.3 × 10^3 g/mol) and Krytox alcohol (average MW = 1.1 × 10^3 g/mol) were both purchased from DuPont and used as received. ^{1}H NMR spectroscopy was performed on a Bruker Avance 400 MHz spectrometer. NMR samples were prepared in $CDCl_3$ (Cambridge Isotope Labs)/TFT or $CDCl_3$/1,1,1,3,3-pentafluorobutane solvent systems. DSC was performed on a Seiko-Haake DSC 220. Samples (∼10 mg) were placed in aluminum pans which were crimped shut. All thermograms were collected from a second heat with a heating rate of 10 °C/min under N_2. The temperature sweep typically ranged from −140 to 150 °C unless otherwise noted.

Synthesis of the Methacryldiamide Perfluoropolyether (Krytox) Macromonomer (PFPED). In a typical synthesis, *N*-(3-aminopropyl)methacrylamide (APMA) hydrochloride (20 g, 140 mmol) was first purified and neutralized according to the procedure reported by Shea et al. and added to a dry 500 mL round-bottom flask.[28] This was followed by the addition of the Krytox methyl ester (60 g, 40 mmol) functional PFPE and ethyl ether (200 mL). The solution was then stirred for 24 h at room temperature. Excess APMA was removed by running the solution through a chromatographic column (alumina, PFB, 2 × 5 cm). Evaporation of PFB yielded a clear, viscous, slightly yellow liquid (62% yield). ^{1}H NMR ($CDCl_3$/TFT): δ = 1.8 ppm (quintet, 2H); δ = 2.0 ppm (singlet, 3H); δ = 3.5 ppm (broad, 4H); δ = 5.4 ppm (singlet, 1H, vinyl); δ = 5.8 ppm (singlet, 1H, vinyl); δ = 6.5 ppm (triplet, 1H, amide); δ = 8.4 ppm (triplet, 1H, amide). ^{19}F NMR: δ = 73.5 ppm (multiplet); δ = 85.5 ppm (multiplet); δ = 88.5 ppm (singlet); δ = 135 ppm (singlet); δ = 136 ppm (singlet); δ = 138 ppm (multiplet).

Synthesis of the Perfluoropolyether (Krytox) Methacrylate Macromonomer (PFPEM). To a 250 mL round-bottom flask with a magnetic stir bar, 20.10 g (17.5 mmol) of Krytox alcohol was

added. This was dissolved in ~100 mL of 1,1,1,3,3-pentafluorobutane (PFB). To this solution 3.2 mL of triethylamine was added (1.3 equiv). The reaction mixture was then degassed for 15 min with a slow Ar(g) purge. The PFB solution was then stirred briskly as 1.7 mL of methacryloyl chloride (17.5 mmol) was slowly added dropwise over 30 min. The reaction was stirred overnight under Ar(g). The reaction was then quenched with a few drops of water. When the resulting evolution of gases subsided, the organic layer was washed with three portions of water and once with brine. The organic layer was separated and diluted with an additional 50 mL of PFB and passed through a silica column. Another 50 mL of PFB was passed through the column in order to flush out any residual product. The solvent was then removed under reduced pressure, leaving the clear PFPE oil (58% yield). ^{1}H NMR ($CDCl_3$/PFB): $\delta = 2.2$ ppm (singlet, 3H); $\delta = 5.0$ ppm (quintet, 2H); $\delta = 5.8$ ppm (singlet, 1H, vinyl); $\delta = 6.5$ ppm (singlet, 1H, vinyl). ^{19}F NMR: $\delta = 73.5$ ppm (multiplet); $\delta = 84.5$ ppm (multiplet); $\delta = 88.5$ ppm (singlet); $\delta = 135$ ppm (singlet); $\delta = 137$ ppm (singlet); $\delta = 138$ ppm (multiplet).

Synthesis of Alkyl (Meth)acrylate-*co*-Glycidyl Methacrylate-*g*-PFPE Terpolymers. In a typical polymerization procedure, ~3 g butyl acrylate (BA) (or methyl methacrylate (MMA)), 3 g of glycidyl methacrylate (GMA), and 4 g of PFPE macromonomer were added to a dry 50 mL round-bottom flask containing a magnetic stir bar. This was followed by addition of 20 mL of a 1:1 PFB/THF solvent mixture and 1 wt % AIBN relative to monomer. The solution was purged for 15 min with Ar(g), immersed in an oil bath maintained at 65 °C, and stirred for 24 h followed by precipitation dropwise into a 10-fold excess of methanol, which is placed in a dry ice/acetone bath. The precipitate was then filtered and dried under reduced pressure. Typical yields ranged between 70% and 90%.

Poly(MMA-*co*-GMA-*g*-PFPED) 3:3:4 Monomer Feed Ratio. Elemental Analysis: Calcd: C, 46.0%; N, 0.77%; O, 23.7%; F, 24.6%; H, 4.9%. Found: C, 47.1%; N, 0.69%; O, 25.6%; F, 21.1%; H, 5.1%. ^{19}F NMR: $\delta = 74.1$ ppm (multiplet); $\delta = 89.5$ ppm (singlet); $\delta = 136$ ppm (singlet); $\delta = 138$ ppm (singlet); $\delta = 139$ ppm (multiplet). GPC (THF): $M_n = 18\,000$; PDI = 2.8. DSC: $T_g(1) = 99$ °C; $T_g(2) =$ unobserved.

Poly(BA-*co*-GMA-*g*-PFPED) 3:3:4 Monomer Feed Ratio. Calcd: C, 47.7%; N, 0.77%; O, 21.6%; F, 24.6%; H, 5.3%. Found: C, 47.7%; N, 0.81%; O, 21.9%; F, 24.5%; H, 5.3%. ^{1}H NMR: $\delta = 0.9$ ppm; $\delta = 1.3$ ppm; $\delta = 1.6$ ppm; $\delta = 2.6$ ppm; $\delta = 2.8$ ppm; $\delta = 3.2$ ppm; $\delta = 3.8$ ppm; $\delta = 4.0$ ppm; $\delta = 4.3$ ppm; $\delta = 1.0-2.5$ ppm (broad multiplet). ^{19}F NMR: $\delta = 74.1$ ppm (multiplet); $\delta = 86$ ppm (multiplet); $\delta = 89.5$ ppm (singlet); $\delta = 136$ ppm (singlet); $\delta = 138$ ppm (singlet); $\delta = 139$ ppm (multiplet). GPC (THF): $M_n = 22\,900$; PDI = 2.3. DSC: $T_g(1) = 7.5$ °C; $T_g(2) = -75$ °C.

Poly(MMA-*co*-GMA-*g*-PFPEM) 3:3:4 Monomer Feed Ratio. Calcd: C, 45.6%; O, 23.9%; F, 25.7%; H, 4.8%. Found: C, 46.8%; O, 25.3%; F, 22.8%; H, 5.0%. ^{19}F NMR: $\delta = 74.1$ ppm (multiplet); $\delta = 89.5$ ppm (singlet); $\delta = 136$ ppm (singlet); $\delta = 138$ ppm (singlet); $\delta = 139$ ppm (multiplet). GPC (THF): $M_n = 20\,000$; PDI = 2.4. DSC: $T_g(1) = 91$ °C; $T_g(2) =$ unobserved.

Poly(BA-*co*-GMA-*g*-PFPEM) 3:3:4 Monomer Feed Ratio. Calcd: C, 47.3%; O, 21.8%; F, 25.7%; H, 5.2%. Found: C, 46.5%; O, 22.4%; F, 26.4%; H, 5.0%. ^{1}H NMR: $\delta = 0.9$ ppm; $\delta = 1.3$ ppm; $\delta = 1.6$ ppm; $\delta = 2.6$ ppm; $\delta = 2.8$ ppm; $\delta = 3.2$ ppm; $\delta = 3.8$ ppm; $\delta = 4.0$ ppm; $\delta = 4.3$ ppm; $\delta = 1.0-2.5$ ppm (broad multiplet). ^{19}F NMR: $\delta = 74.1$ ppm (multiplet); $\delta = 86$ ppm (multiplet); $\delta = 89.5$ ppm (singlet); $\delta = 136$ ppm (singlet); $\delta = 138$ ppm (singlet); $\delta = 139$ ppm (multiplet). GPC (THF): $M_n = 25\,000$; PDI = 2.3. DSC: $T_g(1) = -7.8$ °C; $T_g(2) = -77$ °C.

Photocure of the PFPE Graft Terpolymers. In a typical procedure, the terpolymer (2.0 g) was dissolved in MEK (8 mL) to afford a clear, homogeneous solution at ~20% solids. To this solution 1 wt % (relative to polymer) of WPAG 336 was added and stirred until fully dissolved. The solution was then cast onto glass microscope slides which were then covered under recrystallization dishes, and the solvent was allowed to slowly evaporate for 15 h. Following this, the polymer-coated slides were irradiated in the UV from a mercury arc lamp for 10 min. This is followed by a postexposure bake at 120 °C for 4 h until curing is complete.

Infrared Spectroscopy (IR). IR spectroscopy experiments were performed on a Bio-Rad FTs-7 FTIR spectrometer equipped with a constant temperature heating cell. Samples were cast onto KBr salt plates or glass microscope slides before insertion in to the cell.

Control of Relative Humidity at the Time of Cure. For controlled humidity studies, glass jars were filled with saturated aqueous solutions of KBr, KNO_3, and $NaCr_2O_7 \cdot 2H_2O$.[29] A jar containing fresh Drierite was used as a 0% humidity environment, and a jar containing deionized water was used as a 100% humidity environment. The polymer-coated glass slides were suspended above the aqueous solutions immediately after UV irradiation, and the jar was then tightly sealed. The jars were then placed in an isothermal oven at 80 °C to cure for 24 h.

Dynamic Surface Tensiometry (DST). Tensiometry measurements were performed on a NIMA Technologies DST 9005 dynamic surface tensiometer. Glass coverslips measuring 24 mm × 40 mm × 0.1 mm were coated with un-cross-linked polymer and cured as previously described. The DCA method is based on the Wilhelmy Plate method.[30,31] In a typical experiment, a coated glass coverslip was attached to an electrobalance via a clip, and a stage with a beaker of pure water was automatically raised and lowered to allow the water to impinge upon the slide. Each experiment included multiple immersions to ensure consistent and reproducible data. For all data reported herein we required at least three identical immersions in succession. Through analysis of the resulting force vs distance curves, θ_a and θ_r were obtained. Stage speeds were 100 μm/s.

Settlement and Adhesion Assays with *Ulva* Zoospores. Slides with experimental coatings used in all *Ulva* bioassays were equilibrated in a 30 L tank of recirculating deionized water for 10 days. Slides were transferred to artificial seawater for 2 h before the start of the bioassay. Fertile plants of *Ulva linza* were collected from Wembury Beach, England (50°18′ N; 4°02′ W). Zoospores were released and prepared for attachment experiments. 10 mL aliquots (1.5×10^6 spores mL^{-1}) were pipetted into individual compartments of polystyrene culture dishes (Greiner), each containing a test coating applied to a glass microscope slide. Six replicates of each coating were set up. The dishes were incubated in the dark for 1 h before the slides were washed to remove unattached spores. Three replicate slides from each treatment were fixed in 2% glutaraldehyde in seawater. The remaining three replicates were placed in a flow apparatus.[26] Slides were exposed to a fully developed turbulent flow for 5 min at 53 Pa wall shear stress. After fixing slides in 2% glutaraldehyde, adhered spores were visualized by autofluorescence of chlorophyll and quantified by image analysis as described in ref 25. Thirty counts were taken at 1 mm intervals along the middle of the long axis of each of the three replicate slides. Spore settlement data are expressed as the mean number of spores adhered per mm^2 ± 95% confidence limits ($n = 90$). The adhesion strength data were calculated from the mean number of spores remaining attached to the surface after exposure to turbulent flow compared with the mean number before the slides were subjected to flow. Data are presented in terms of percent spore removal compared with the controls, ± standard errors calculated from arcsine-transformed data. Two standards were included in all assays: acid-washed glass and a poly(dimethylsiloxane) elastomer (PDMSE), T2 Silastic (Dow Corning). The slides with coatings of T2 Silastic were supplied by Professor A. B. Brennan at the University of Florida. The samples thus provided were prepared as described in previous publications.[32] Details regarding the cure chemistry and specific composition of the Silastic T-2 base resin and curing agent as received from the manufacturer are reported elsewhere.[33]

Adhesion Assays with *Ulva* Sporelings. Experiments were also conducted on sporelings, i.e., young plants that develop from attached spores, as described in ref 34. After 8 days of growth, biomass was estimated by measurement of fluorescence from chlorophyll a contained within the cells of the young plants using

a Tecan plate reader. Ninety readings were taken before and after exposure of six replicates slides to a wall shear stress of 53 Pa. The water channel produced fully developed turbulent flow similar to that experienced around the hull of a ship traveling at 15 knots. Data are presented in terms of percent sporeling removal compared with the controls, ±95% confidence limits from arcsine-transformed data. Acid-washed glass and T2 Silastic were included as standards in all assays.

Results and Discussion

We have an interest in the development of minimally adhesive nontoxic foul-release coatings, for utility in applications that range from ship hull coatings to medical devices. There is increasing interest as to the various practical and synthetic considerations which may hold significant sway over the surface composition, wettability, and adhesion characteristics of polymeric materials such as those targeted herein. To determine the ideal chemical and mechanical properties for fouling release coatings, several series of materials were generated in order to isolate various properties and optimize PFPE surface enrichment. Synthetically, a modular macromonomer approach was employed allowing for direct structure/property correlations. The basic design was a random terpolymer with three variable monomer classes. The first monomer class was an alkyl (meth)acrylate, specifically, either butyl acrylate (BA) or methyl methacrylate (MMA). These monomers were chosen due to the very different (high and low) T_gs exhibited by their respective homopolymers. This provides a means of isolating the effect of modulus and T_g on the observed surface and wetting properties, while the basic chemical nature of the monomer remained unchanged. The second monomer class contained a curable functional group. Through variation of composition and curing conditions, the relative effect of cross-link density was evaluated. Glycidyl methacrylate was chosen as the curable monomer for these polymers. The third monomer class was the PFPE macromonomer itself. The incorporation of this monomer provided for a highly surface active, low-energy, fluorinated component. The low surface tensions associated with fluoropolymers provide a driving force for the observed surface enrichment of the PFPE domains in these studies.[8] Indeed, because of this phenomenon, fluoropolymers have often been studied and applied as surface-modifying components in such applications as coatings and lubricants.[16] Additionally, polymer surfaces rich in fluorinated functional groups can be envisioned to express other properties upon the solid surface, such as resistance to chemicals and organic solvents, hydrophobicity, and a low coefficient of friction.

Macromonomer and Terpolymer Synthesis. We also set out to investigate the effect of the chemical nature of the polymerizable "linker" group corresponding to the macromonomer on the surface dynamics of these materials. To this end, two macromonomers (as named in the Experimental Section), differing only in the nature of the polymerizable end group, were synthesized. The *N*-(3-aminopropyl)methacrylamide PFPE macromonomer (PFPED) was synthesized readily through the neutralization of *N*-(3-aminopropyl)methacrylamide (APMA) hydrogen chloride with a slight excess of sodium ethoxide and the subsequent amidation of the methyl ester Krytox (MW = 1.3×10^3) with the resulting APMA base (Scheme 1). This provided a PFPE macromonomer graft with a polymerizable methacryldiamide end group (PFPED).

A second, less polar, PFPE methacrylate macromonomer was synthesized by the reaction of the Krytox alcohol (MW = 1.1×10^3) PFPE with a stoichiometric amount of methacryloyl chloride (Scheme 2). Both synthetic procedures are straightforward and provided each macromonomer in high yields.

Scheme 1. Synthetic Details of the APMA Krytox Macromonomer (PFPED)

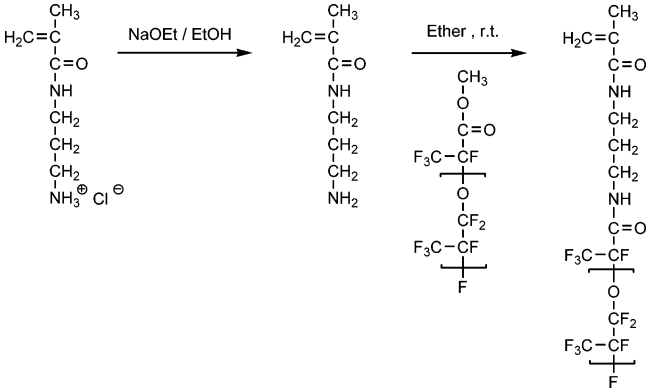

Scheme 2. Synthetic Details of the Krytox Methacrylate Macromonomer (PFPEM)

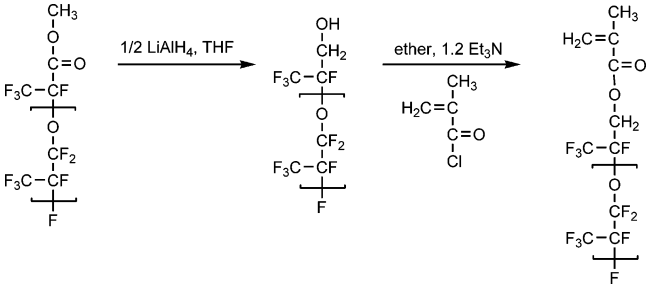

Scheme 3. Synthetic Details of the PFPE Graft Terpolymers[a]

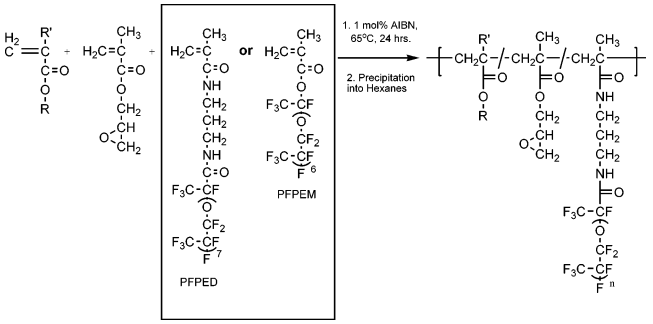

[a] R = R′ = Me (methyl methacrylate); R = *n*-butyl, R′ = H (butyl acrylate); modulus handle. The glycidyl methacrylate provides a means of curing the samples photolytically by use of a photoacid generator (PAG) (Scheme 4).

Terpolymer Synthesis. Each terpolymer was synthesized through a free radical polymerization of the described monomers having a feed ratio of 3:3:4 for the alkyl (meth)acrylate, glycidyl methacrylate, and PFPE macromonomer, respectively, by weight. The reactions were carried out in a 1:1 PFB/THF solvent mixture using 1 wt % AIBN relative to monomer feed as the initiator. For the purposes of this study, four terpolymers were synthesized such that each of the two "linker" chemistries could be explored within both high and low modulus matrices. The details of the syntheses are illustrated in Scheme 3.

These reactions produced the targeted, random PFPE graft terpolymers with compositions closely matching those of the initial feed ratios of all three monomers as measured by ^{1}H NMR and elemental analysis. GPC data collected against polystyrene standards for each of the four terpolymers exhibited monomodal distributions with comparable elution times corresponding to number-average molecular weights between approximately 20 000 and 25 000 with polydispersities of around 2.5 (Table

Table 1. Structural and Thermal Properties of the PFPE Graft Terpolymers

	GPC[b]		DSC[c]		TGA[d]	composition by weight (%)[e]	
sample[a]	M_n ($\times 10^4$)	M_w/M_n	T_g^1 (°C)	T_g^2 (°C)	T_d (°C)	PFPED	PFPEM
1	2.3	2.3	7.5	−75	315	39	
2	2.5	2.3	−7.8	−77	230		42
3	1.8	2.8	99		260	34	
4	2.0	2.4	91		180		36

[a] Sample 1, poly(BA-*co*-GMA-*g*-PFPED); sample 2, poly(BA-*co*-GMA-*g*-PFPEM); sample 3, poly(MMA-*co*-GMA-*g*-PFPED); sample 4, poly(MMA-*co*-GMA-*g*-PFPEM). [b] Molecular weights were measured against polystyrene standards. [c] Low-temperature transitions (T_g^2) were only observed for the butyl acrylate-based terpolymers. [d] Listed values for T_d were taken at 5% weight loss. [e] Listed weight fractions of the PFPE component were calculated from elemental analysis data.

Scheme 4. Details of the Photolytic Acid-Catalyzed Epoxide Ring-Opening Cure Chemistry Employed for the PFPE Graft Terpolymer Films

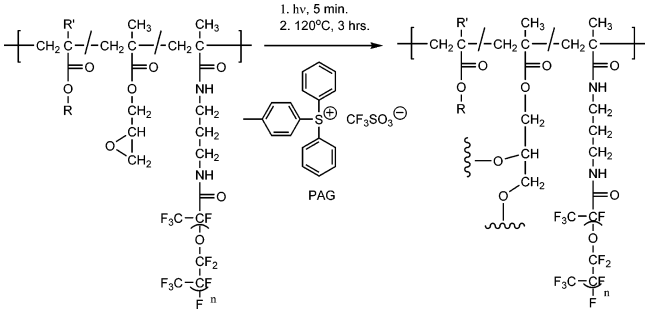

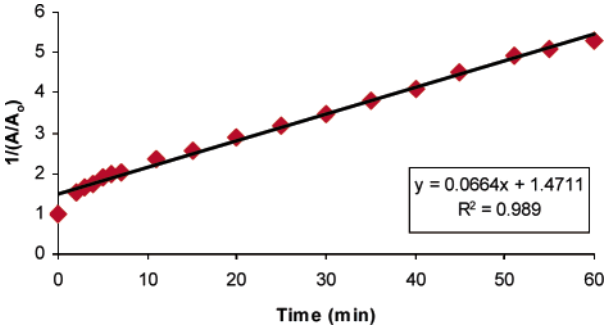

Figure 2. IR absorbance data fit to a second-order rate expression for the epoxy cure.

1). Therefore, these four polymers are observed to exhibit comparable molecular weights with nearly identical compositions with respect to each monomer class previously described.

Cure Chemistry. Films of these polymers were cast from MEK solutions (20 wt % in polymer) containing 1 wt % of a photoacid generator (WPAG 336, Scheme 4). Upon UV irradiation, an organic acid is generated which catalyzes the ring-opening of the epoxy pendant groups from the incorporated glycidyl methacrylate comonomer. The details of this chemistry are illustrated in Scheme 4.

Thermal Analysis: DSC. DSC data were gathered for this series of samples. These showed two distinct glass transition temperatures (labeled T_g^1 and T_g^2). The T_g of the pure PFPE macromonomer itself was found to be −71 °C. Thus, the low-temperature transitions (T_g^2) are ostensibly attributed to the PFPE-rich domains. These data are consistent with a heterogeneous, phase-separated morphology. Similar results were observed by Möller et al.[35] and Bongiovanni et al.[36] for related systems.

Dynamic Wetting Characteristics before and after Cure. The initial focus of the study was confined to the two BA-based polymers, poly(BA-*co*-GMA-*g*-PFPED and -PFPEM) (i.e., none of the high-T_g MMA-based terpolymers). Additionally, we observed that although advancing contact angles were rather high (∼117°), as expected, the receding contact angles were consistently and significantly lower than the advancing angles (by 40° at best) for the poly(BA-*co*-GMA-*g*-PFPED) coatings. As was mentioned previously, contact angle hysteresis provides an implicit indication of the relative degree of interaction across the liquid/solid interface. As such, our interpretation is that the low receding contact angles (θ_r), relative to θ_a, are an indication of significant surface restructuring. This is presumably due to the presence of high-energy moieties (i.e., the diamide groups) within the polyacrylate structure and the associated propensity to migrate to the surface when in contact with the high-energy medium. To test this hypothesis, the degree to which the chemical nature of the "linker" group corresponding to the PFPE macromonomer graft affects the observed surface dynamics of such a terpolymer upon contact with an aqueous surrounding medium has been explored. Acting on the assumption that less polar chemistries (i.e., methacryl ester) would serve to minimize the driving force for domain segregation, polymers incorporating both the PFPEM and PFPED grafts have been evaluated in parallel. Further, the extent to which the degree of cure affects chain mobility at the interface and consequently the observed surface reorganization upon wetting was also determined.

To address these issues, films of poly(BA-*co*-GMA-*g*-PFPED) and poly(BA-*co*-GMA-*g*-PFPEM) were prepared by dip-coating a series of glass coverslips in methyl ethyl ketone (MEK) casting solutions (including the PAG 1 wt % relative to polymer). The films were cured by irradiation with a mercury arc lamp for 5 min (generating the acid) followed by a postexposure bake at 120 °C (Scheme 4).

An evaluation of the kinetics of the acid-catalyzed epoxy cure was undertaken. IR spectroscopy was used to monitor the curing reaction and extrapolate kinetic data (the details of this are described in the Experimental Section). The cure chemistry was readily observed through observation of the band at 908 cm^{-1} associated with the epoxy pendant group of the GMA comonomer. Spectra were recorded every few minutes throughout the reaction, and the time-dependent decay of this peak was evaluated. It was observed that the peak does not decrease to zero absorbance. However, this is presumably due to restricted chain movement at high cross-link densities. From these data, a kinetic analysis of this curing reaction was obtained (Figure 2). It was found that the ring-opening reaction of the epoxy group obeyed a second-order rate law with a rate constant of 0.07 min^{-1}. Further, it was determined that the maximum cross-link density for this system was obtained after only 3 h bake time following irradiation.

With a clear picture of the cure system in hand, the evaluation of CA's as a function of cross-link density was undertaken. Film samples of the poly(BA-*co*-GMA-*g*-PFPED) and poly(BA-*co*-GMA-*g*-PFPEM) were prepared, irradiated, and subjected to postexposure bakes (T = 120 °C) for various times ranging from 5 to 180 min (3 h bakes being necessary to accomplish a complete cure as illustrated by the kinetic data). At regular

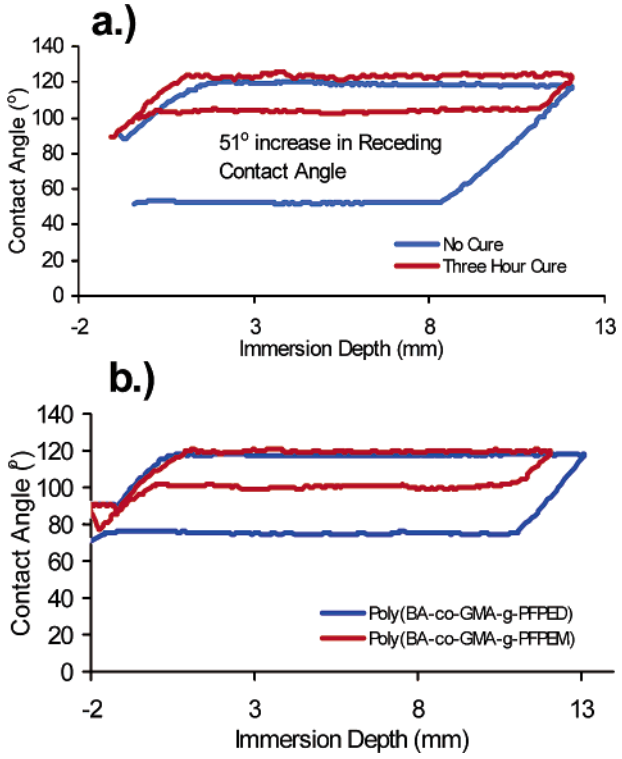

Figure 3. Tensiometry data (contact angle vs immersion depth). (a) Contact angle data collected for poly(BA-*co*-GMA-*g*-PFPEM) before and after cure (postexposure bake at 120 °C overnight). The receding contact angle increased by 51° upon curing. (b) Contact angle data collected for both poly(BA-*co*-GMA-*g*-PFPEM and -PFPED) after cure (postexposure bake at 120 °C overnight). The observed hystereses were $18 \pm 2°$ and $42 \pm 2°$, respectively. The observed receding contact angles for poly(BA-*co*-GMA-*g*-PFPED) are ~50° prior to cure.

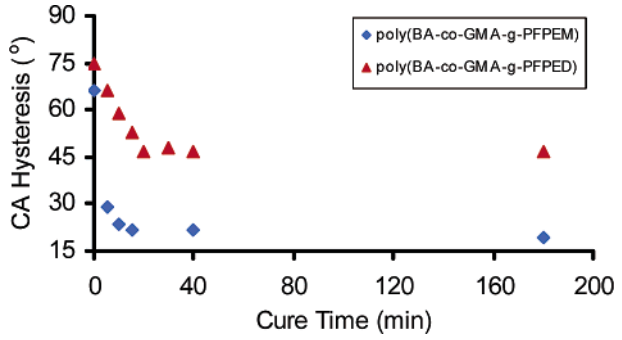

Figure 4. Contact angle hysteresis exhibits a pronounce decay with postexposure bake time (120 °C). The data points at 0 min are the values for the sample films that were not cured. It is worth noting that the sample incorporating the PFPEM graft provides for a hysteresis measured 10° less than that for the PFPED-based polymer films.

intervals samples were removed from the oven, and curing was quenched by immersion into liquid nitrogen. Each cured film was evaluated by dynamic surface tensiometry (details are described in the Experimental Section) as to θ_a, θ_r, and ($\theta_a - \theta_r$). The results are given in Figures 3 and 4.

Figure 3 outlines the tensiometry data collected for both poly(BA-*co*-GMA-*g*-PFPED) and poly(BA-*co*-GMA-*g*-PFPEM). Plots a and b present the contact angle data collected via the Wilhelmy plate method for the BA-based polymers before and after cure (postexposure bakes were applied overnight). Inspection of these data clearly demonstrates the significant influence of cross-link density on the observed CA hysteresis. Further, the receding contact angle is sensitive to the cure state of the polymer, while advancing angles remain essentially constant, any deviation of which is well within the statistical error of the experiment. Figure 4 illustrates the decay in CA hysteresis as a function of postexposure bake time. These data are given for both poly(BA-*co*-GMA-*g*-PFPED) and poly(BA-*co*-GMA-*g*-PFPEM). The data in Figure 4 serve to further underscore the pronounced restrictive effect of cross-link density upon the surface dynamics of these polymer systems. Additionally, the decay in hysteresis with cure time follows precisely with the decay of the 908 cm^{-1} band from the previously described vibrational spectroscopy analysis of the cure chemistry (Figure 2). It should be noted that recently Ober and co-workers reported a significant decrease in CA hysteresis as a result of annealing a semifluorinated graft copolymer without the need for chemical cross-linking. However, the polymer system in question exhibited a liquid crystalline smectic phase at the surface which was reported to contribute significantly to the inhibition of surface reconstruction under water.[37] As such, this study offers additional examples of the controlled inhibition of surface dynamics by physical or chemical means.

It is further evident from these data that the increase in θ_r with cross-link density is far more pronounced for the poly(BA-*co*-GMA-*g*-PFPEM) films. Also, it is apparent that there is a reduced hysteresis (66° vs 75°) for these films prior to cure. All of these data are entirely consistent and support the assertion that a less polar "linker" chemistry reduces the driving force for domain segregation from the surface and that cross-link density serves to restrict chain mobility and by extension surface restructuring upon wetting by a high-energy liquid. It is further evident that these parameters may be manipulated in order to generate a surface that exhibits more "ideal" behavior, all other considerations being equal.

Given the observations regarding cross-link density, it naturally follows that T_g should have a significant influence on surface dynamics as well. To explore this issue, it was necessary to prepare two additional terpolymers of the type poly(MMA-*co*-GMA-*g*-PFPE), incorporating methyl methacrylate (MMA) rather than butyl acrylate. MMA was chosen in order to provide a glassy material at room temperature without introducing any significant differences in the chemical composition of the resulting terpolymers. DSC analysis provided T_gs of ~−5 and ~95 °C for the BA- and MMA-based terpolymer analogues, respectively (actual values for each of the four terpolymers are given in Table 1).

Once synthesized and characterized, the two MMA-based terpolymers were used to prepare MEK film-casting solutions in an identical fashion as previously described. These solutions were used to dip-coat glass slides in order to provide film samples. The films are then irradiated for 5 min under the mercury arc lamp as before and subjected to a postexposure bake at 120 °C overnight to provide completely cured films. These films were characterized by DST analysis in an identical fashion as the BA-based terpolymers. Figure 5 presents the CA data for both poly(MMA-*co*-GMA-*g*-PFPED) and poly(MMA-*co*-GMA-*g*-PFPEM) as observed after complete cure of the films. It is immediately evident upon inspection that the CA hysteresis is observed to be far less pronounced for poly(MMA-*co*-GMA-*g*-PFPED) than that observed for the BA-based analogue. Indeed, the hysteresis values are 24° and 20° for the poly(MMA-*co*-GMA-*g*-PFPED and −PFPEM) terpolymers, respectively. There is only a 4° difference in the two hysteresis measurements, and consistently, the greater of the two values is associated with the PFPED-incorporated polymer. These data are quite demonstrative of the restricted chain mobility observed in the polymethacrylate glass. In fact, it appears that the higher T_g serves to further enhance the observed receding CA for the

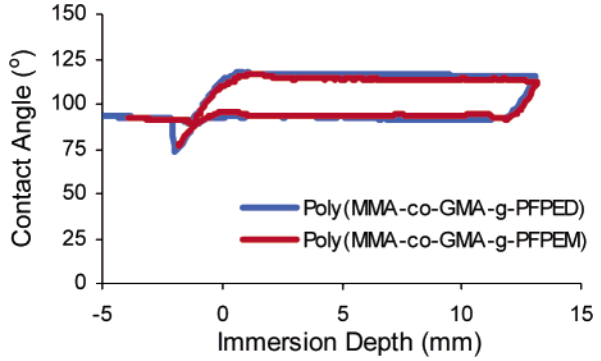

Figure 5. Contact angle data for the two MMA-based polymer films (postcure). The two materials observe contact angle hystereses of 24° and 20° for poly(MMA-*co*-GMA-*g*-PFPED) and poly(MMA-*co*-GMA-*g*-PFPEM) films, respectively.

Table 2. Relative Humidities at 80 °C Associated with Saturated Aqueous Solutions of Various Salts

salt	% relative humidity at 80 °C[a]
none (pure water)	100
KBr	79.5
$NaNO_3$	65.5
$NaCr_2O_7 \cdot 2H_2O$	56.0
Drierite (no solution)	0.0

[a] The % relative humidity is defined as (vapor pressure/saturation pressure) × 100%.

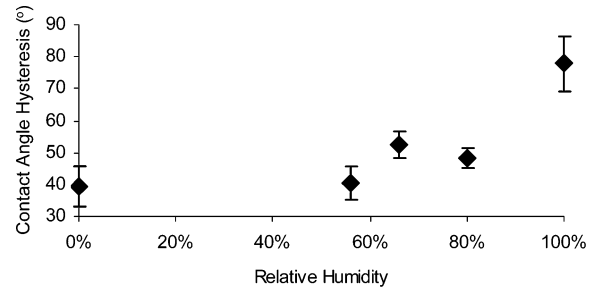

Figure 6. Contact angle hysteresis observations collected for poly(BA-*co*-GMA-*g*-PFPED) cured under a postexposure bake temperature of 80 °C while suspended in a closed vessel above saturated aqueous solutions of the various salts listed in Table 1.

poly(MMA-*co*-GMA-*g*-PFPED) film by 20° relative to that observed for the BA-based analogue.

Finally, as these coatings are observed to exhibit various sensitivities to the nature of the surrounding medium, an investigation as to the effect of relative humidity at the time of cure was undertaken. In other words, could relative humidity or the lack of moisture in the atmosphere at the time of cure be used to drive an ever higher surface enrichment of PFPE, and once so segregated, would the surface be "locked" into that morphology as a consequence of the resulting cure state? To this end, a series of five films were dip-coated on glass substrates as before. These were irradiated and then suspended in airtight glass vessels, above saturated aqueous solutions of various salts, each producing a known relative humidity within the vessel at a given temperature (80 °C in the case of these experiments) (Table 2).[38] Contact angle hysteresis measurements are summarized in Figure 6 as a function of relative humidity. Reduction of the relative humidity from 100% to 0% resulted in a 40° (50%) decrease in the observed contact angle hysteresis for the samples tested. Control experiments were performed using the poly(GMA-*co*-BA) copolymer (30 wt % GMA). These materials were completely insensitive to the relative humidity of the curing environment and showed no change in advancing or receding contact angle. The results of this study clearly show that the

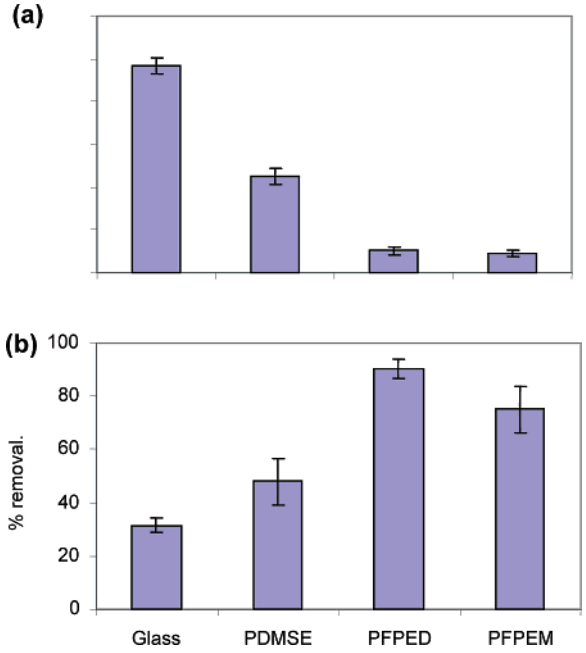

Figure 7. (a) Number of spores mm^{-2} attached to the surface of poly(MMA-*co*-GMA-*g*-PFPED) and poly(MMA-*co*-GMA-*g*-PFPEM) compared to the glass and PDMSE (T2 Silastic) standards. Each point is the mean of 90 counts, 30 from each of 3 replicates; bars show 95% confidence limits. (b) Percentage removal of spores from the surface of poly(MMA-*co*-GMA-*g*-PFPED) and poly(MMA-*co*-GMA-*g*-PFPEM) compared to the glass and PDMSE (T2 Silastic) standards. Each point is derived from the mean of 90 counts before and after exposure to a wall shear stress of 53 Pa in a water channel. Bars show 95% confidence limits from arcsine transformed data.

PFPE terpolymers are highly sensitive to relevant environmental parameters at the time of cure and further suggest that postexposure bake temperatures well in excess of 100 °C are preferred in order to minimize CA hysteresis.

Figure 7a shows the number of spores settled on the two test surfaces and the glass and PDMSE standards. The number of spores on both test surfaces was markedly less than on either of the two standards, being approximately 10% and 25% of glass and the PDMS elastomer (T-2 Silastic), respectively. The ease with which the spores were removed by the application of a wall shear stress of 53 Pa is shown in Figure 7b. Percentage removal from both test surfaces was greater than from the T-2 Silastic standard, highest removal being from the poly(MMA-*co*-GMA-*g*-PFPED) film.

In addition to spore settlement and release, the fouling release potential was further measured through evaluation of the ease by which 8 day old sporelings (a more mature stage of development in the *Ulva* lifecycle) were removed from the surface. Percentage removal is shown in Figure 8. While removal from both of the perfluoroether-based graft terpolymers was less than from that of a standard fouling release silicone (T2 Silastic), the poly(MMA-*co*-GMA-*g*-PFPED) coatings shows some promise as a fouling release material. However, it is clear that further optimization will be required. Further modifications to these graft terpolymers are under way, and results are forthcoming.

Conclusions

We have demonstrated the critical parameters that influence or drive the evolution of "surface states" for a series of heterogeneous, cross-linkable, random PFPE graft terpolymers: interfacial free energy, chain mobility (T_g and cross-link density), and intermolecular interactions with the surrounding

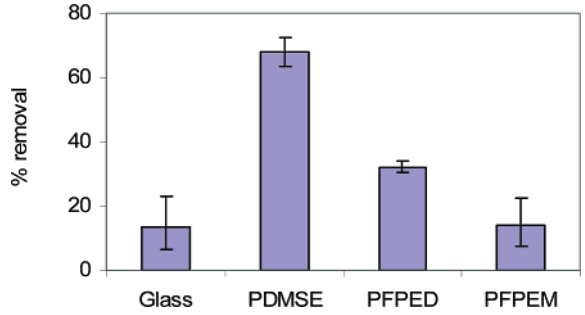

Figure 8. Percentage removal of 8 day sporelings from the surface of poly(MMA-*co*-GMA-*g*-PFPED) and poly(MMA-*co*-GMA-*g*-PFPEM) compared to the glass and PDMSE (T2 Silastic) standards. Each point is derived from the mean of 90 fluorescence counts on each of 6 replicate slides before and after exposure to a wall shear stress of 53 Pa in a water channel. Bars show 95% confidence limits from arcsine transformed data.

media. Throughout the course of these studies we have sought to take advantage of the utility of random copolymers in the development of coatings with control of specific properties. Our initial interest in minimally adhesive, fouling release applications prompted our focus on to surface-enriched PFPE graft terpolymer coatings. Because large observed hysteresis in dynamic water contact angle measurements has been associated with increased adhesion,[39] it is important to understand those considerations which serve to minimize this hysteresis in a predictable way. With an understanding of the chemical and thermodynamic driving forces for the evolution of "surface states" in various surrounding media, we demonstrated that dynamic surface processes can be manipulated (or mitigated) in a controlled way by various means. We first demonstrated that restriction of the free segmental motion of the polymer chains could severely curtail surface reconstruction upon wetting by an aqueous medium. The "cure-state-dependent" evolution of contact angle hysteresis was demonstrated (Figure 4). Additionally, it was shown that θ_a (initial state) was virtually insensitive to cross-link density (Figure 3). A corollary to this is that high-T_g materials are less susceptible to surface reconstruction and by extension CA hysteresis (Figure 5). Additionally, we have demonstrated that employing monomers with highly polar chemistries will, upon immersion, serve to promote favorable intermolecular interactions with the high-energy aqueous medium, further enhancing the driving force for segregation of the PFPE domains from the surface (Figure 3b). The biological data indicate that these materials, especially the poly(MMA-*co*-GMA-*g*-PFPED) coating, show promise as both fouling-resistant and fouling-release materials.

Acknowledgment. This research is supported by the Office of Naval Research under Grant N00014-02-1-0185 to J.M.D. and Grant N00014-02-1-0521 to J.A.C. and M.E.C. J.M.D. also acknowledges the NSF-STC Center for Environmentally Responsible solvents and Processes for shared facilities. The authors thank David Snead, Johnaustin Chapman, Dr. Derek Schorzman, and Dr. Lori Hermann for helpful discussions and assistance in the laboratory.

References and Notes

(1) Langmuir, I. *Science* **1938**, *87*, 493.
(2) (a) Yasuda, H.; Charlson, E. J.; Charlson, E. M. *Langmuir* **1991**, *7*, 2394−2400. (b) Yasuda, T.; Miyama, M.; Yasuda, H. *Langmuir* **1992**, *8*, 1425−1430. (c) Yasuda, T.; Miyama, M.; Yasuda, H. *Langmuir* **1994**, *10*, 583−585.
(3) Mansky, P.; Liu, Y.; Huang, E.; Russell, T. P.; Hawker, C. *Science* **1997**, *275*, 1458 and references therein.
(4) Genzer, J.; Efimenko, K. *Science* **2000**, *290*, 2130 and references therein.
(5) Wu, S. *Polymer Interface and Adhesion*; Marcel Dekker: New York, 1982.
(6) Garbassi, F.; Morra, M.; Occhiello, E. *Polymer Surfaces: From Physics to Technology*; John Wiley and Sons: New York, 1994.
(7) Carey, D. H.; Grunzinger, S. J.; Ferguson, G. S. *Macromolecules* **2000**, *33*, 8802 and references therein.
(8) Garrett, J. T.; Runt, J.; Lin, J. S. *Macromolecules* **2000**, *33*, 6353 and references therein.
(9) (a) Chen, W.; McCarthy, T. J. *Macromolecules* **1999**, *32*, 2342 and references therein. (b) Cross, E. M.; McCarthy, T. J. *Macromolecules* **1990**, *23*, 3916 and references therein.
(10) (a) Elman, J. F.; Johns, B. D.; Long, T. E.; Koberstein, J. T. *Macromolecules* **1994**, *27*, 541 and references found therein. (b) Koberstein, J. T. In *Encyclopedia of Polymer Science and Engineering*, 2nd ed.; Mark, H. F., Bikales, N. M., Overberger, C. G., Menges, G., Kroschwitz, J. I., Eds.; John Wiley and Sons: New York, 1989; Vol. 8, p 237.
(11) Hunt, M. O.; Belu, A.; Linton, R.; DeSimone, J. M. *Macromolecules* **1993**, *26*, 4854.
(12) Iyengar, D. R.; Perutz, S. M.; Dai, C.; Ober, C. K.; Kramer, E. J. *Macromolecules* **1996**, *29*, 1229 and references therein.
(13) Throughton, E. B.; Bain, C. D.; Whitesides, G. M.; Nuzzo, R. G.; Allara, D. L.; Porter, M. D. *Langmuir* **1988**, *4*, 365.
(14) Bain, C. D.; Whitesides, G. M. *Science* **1988**, *240*, 62.
(15) Young's equation: Young, T. *Philos. Trans. R. Soc. London* **1805**, 65.
(16) Scheirs, J. *Modern Fluoropolymers*; John Wiley & Sons, Ltd.: New York, 1997.
(17) (a) Rolland, J. P.; Hagberg, E. C.; Denison, G. M.; Carter, K. R.; DeSimone, J. M. *Angew. Chem., Int. Ed.* **2004**, *43*, 5796−5799. (b) Rolland, J. P.; Maynor, B. W.; Euliss, L. E.; Exner, A. E.; Denison, G. M.; DeSimone, J. M. *J. Am. Chem. Soc.*, in press. (c) Rolland, J. P.; Van Dam, R. M.; Schorzman, D. A.; Quake, S. R.; DeSimone, J. M. *J. Am. Chem. Soc.* **2004**, *126*, 2322−2323.
(18) Townsin, R. L. *Biofouling* **2003**, *19 (*Suppl.*)*, 9−15.
(19) Kavanagh, C. J.; Schultz, M. P.; Swain, G. W.; Stein, J.; Truby, K.; Darkangelo-Wood, C. *Biofouling* **2001**, *17*, 155−167.
(20) Stein, J.; Truby, K.; Darkangelo-Wood, C.; Takemori, M.; Vallance, M.; Swain, G.; Kavanagh, C.; Kovach, B.; Schultz, M.; Wiebe, D.; Holm, E.; Montemarano, J.; Wendt, D.; Smith, C.; Meyer, A. *Biofouling* **2003**, *19*, 87−94.
(21) Sun, Y.; Guo, S.; Walker, G. C.; Kavanagh, C. J.; Swain, G. W. *Biofouling* **2004**, *20*, 279−289.
(22) Brady, R. F.; Singer, I. L. *Biofouling* **2000**, *15*, 73−81.
(23) Berglin, M.; Lönn, N.; Gatenholm, P. *Biofouling* **2003**, *19* (Suppl.), 63−69.
(24) Singer, I. L.; Kohl, J. G.; Patterson, M. *Biofouling* **2000**, *16*, 301−309.
(25) Finlay, J. A.; Callow, M. E.; Schultz, M. P.; Swain, G. W.; Callow, J. A. *Biofouling* **2002**, *18*, 251−256.
(26) Schultz, M. P.; Finlay, J. A.; Callow, M. E.; Callow, J. A. *Biofouling* **2000**, *15*, 243−251.
(27) Schultz, M. P.; Finlay, J. A.; Callow, M. E.; Callow, J. A. *Biofouling* **2003**, *19 (*Suppl.*)*, 17−26.
(28) Shea, K. J.; Spivak, D. *J. Org. Chem.* **1999**, *64*, 4627−4634.
(29) Dean, J. A. *Lange's Handbook of Chemistry*, 15th ed.; McGraw-Hill: New York, 1998.
(30) Johnson, R. E.; Dettre, R. H. In *Surfactant Science Series*; Berg, J. C., Ed.; Marcel Dekker: New York, 1997.
(31) Adamson, A. W.; Gast, A. P. In *Physical Chemistry of Surfaces*, 6th ed.; John Wiley and Sons: New York, 1993; Vol. 49, pp 1−73.
(32) Hoipkemeier-Wilson, L.; Schumacher, J. F.; Carman, M. L.; Gibson, A. L.; Feinberg, A. W.; Callow, M. E.; Finlay, J. A.; Callow, J. A.; Brennan, A. B. *Biofouling* **2004**, *20*, 53−63.
(33) Wilson, L. H. Bioresponse to Polymeric Substrates: Effect of Surface Energy, Modulus, Topography and Surface Graft Copolymers. Ph.D. Dissertation, University of Florida, Gainesville, FL, 2005.
(34) Chaudhury, M. K.; Finlay, J. A.; Chung, J. Y.; Callow, M. E.; Callow, J. A. *Biofouling* **2005**, *21*, 41−48.
(35) Krupers, M.; Möller, M. *Macromolecules* **1998**, *31*, 2552−2558.
(36) Bongiovanni, R.; Malucelli, G.; Lombardi, V.; Priola, A.; Siracusa, V.; Tonelli, C.; Di Meo, A. *Polymer* **2001**, *42*, 2299−2305.
(37) Krishnan, S.; Ober, C. K.; Ayothi, R.; Lin, Q.; Paik, M.; Hexemer, A.; Kramer, E. J.; Fischer, D. *Polym. Prepr.* **2005**, *46*, 613−614.
(38) Dean, J. A. *Lange's Handbook of Chemistry*, 15th ed.; McGraw-Hill: New York, 1998.
(39) Schmidt, D. L.; Brady, Jr., R. F.; Lam, K.; Schmidt, D. C.; Chaudhury, M. K. *Langmuir* **2004**, *20*, 2830−2836.

MA0524777